The oxidative coupling of methane and the activation of molecular O_2 on CeO_2/BaF_2 ☆

X.P. Zhou, Z.S. Chao, W.Z. Weng, W.D. Zhang, S.J. Wang, H.L. Wan and K.R. Tsai

Department of Chemistry, Xiamen University, Xiamen 361005, PR China

Received 24 March 1994; accepted 3 August 1994

CeO_2/BaF_2 was used as the catalyst for the oxidative coupling of methane (OCM). At 800°C and $CH_4 : O_2 = 2.7 : 1$, CH_4 conversion of 34% with C_2 hydrocarbon selectivity of 54.3% was obtained. XRD measurement showed that partial anion (O^{2-}, F^-) and/or cation (Ce^{4+}, Ba^{2+}) exchange between CeO_2 and BaF_2 lattices occurred. ESR study showed that O^- species existed on degassed catalyst. XPS study revealed that, when BaF_2 was added to CeO_2, the binding energy of Be $3d_{5/2}$ was 2.2 eV lower than that in CeO_2, and the "electron-enriched lattice oxygen" species was detected. XPS, ESR and Raman study showed that, under O_2 adsorbing conditions, O_2^{2-} and O_2^- species were detected on CeO_2/BaF_2.

Keywords: OCM; metal oxide–fluoride; electron-enriched lattice oxygen; quasi-free electrons.

1. Introduction

In the investigation of the OCM reaction, various catalysts were developed. Most of them are composite metal oxide or metal carbonate catalysts, as well as Cl^-, Br^- promoted metal oxide catalysts [1–3]. F^- ion modified catalysts are seldom studied. In the last two years, we have developed a novel series of F^- anion promoted metal oxide–fluoride catalysts [3–6], and studied the possible mechanisms for the formation of active centers and activation of molecular oxygen on these catalysts. In this paper, we report recent studies on the OCM reaction, the formation of active centers and the activation of O_2 over CeO_2/BaF_2 catalyst.

2. Experimental

The catalysts used in our experiment were prepared by mixing CeO_2 with BaF_2 or CeO_2 with BaO according to the molar ratios listed in table 1.

☆ This work was supported by the State Key Laboratory for Physical Chemistry of the solid surface and the National Science Foundation of China.

Table 1
The composition of catalysts

	CB1	CB2	CB3	CB4	CB5	CB8
$CeO_2 : BaF_2$	1 : 1	1 : 2	1 : 3	1 : 4	1 : 5	1 : 8
	CBO1	CBO2	CBO3	CBO4	CBO5	
$CeO_2 : BaO$	1 : 1	1 : 2	1 : 3	1 : 4	1 : 5	

The mixtures were stirred with water. The wet mixtures were then dried at 100°C for 1 h and calcined at 900°C for 6 h. After the calcination, CBO1 to CBO5 became melted solid state material. The resulting solids were then crushed and sieved to 40–80 mesh particles.

The catalytic evaluation was carried out in a fixed-bed quartz reactor equipped with a gas chromatograph. All data were obtained after 6 h on stream.

The X-ray diffraction patterns were determined on a Rigaku Rotaflex D/Max-C instrument equipped with a wide-angle goniometer and using Cu Kα radiation.

The samples used in XPS, Raman and ESR characterization were treated in a flow of helium at 900°C for 30 min, followed by H_2 at the same temperature for 30 min. After the above treatment, the sample was purged with helium under atmospheric pressure at 900°C for 10 min, and cooled under helium to room temperature. Half of the catalyst was separated and sealed in a glass tube under He atmosphere to obtain the degassed sample. The rest of the sample was exposed to O_2 at room temperature, then purged with He to remove gas phase O_2 and then sealed in a glass tube in helium to obtain the O_2 adsorbed sample.

The XPS measurement of the O_2 adsorbed sample was carried out at room temperature on an ESCALAB MKII XPS instrument with Al Kα radiation ($h\nu = 1486.6$ eV) under a pressure $P < 1 \times 10^{-8}$ Torr. The sample tube was broken in the sample treatment chamber of the spectrometer and then transferred to the analysis chamber for spectrum recording. The spectra were referenced to the C 1s peak at 284.6 eV.

The Raman measurement was carried out on a U-1000 Raman spectrometer at room temperature. The laser wavelength was 5145 Å. The scanning region ranged from 600 to 1500 cm^{-1}.

The ESR analysis of the degassed and O_2 adsorbed samples was carried out on a Bruker ESR spectrometer at room temperature.

3. Results and discussion

From table 2, it was found that, under the reaction conditions, BaF_2 has no activity for the OCM reaction, and CeO_2 was actually a complete combustion catalyst for CH_4 oxidation. Possibly because of the reaction of BaO with H_2O to produce $Ba(OH_2)$, which melted in the calcining process at 900°C leading to a decrease

Table 2
Catalytic performance at 800°C, $CH_4 : O_2 = 2.7 : 1$, GHSV = 15000 h^{-1}

Catalyst	CH_4 conv.	Selectivity (%)					Yield (%)	Specific surface area (m^2/g)
		CO	CO_2	C_2H_4	C_2H_6	C_2		
BaF_2	0						0	
CeO_2	24.3	19.7	74.0	3.35	2.86	6.21	1.51	
CB1	32.76	0	48.06	31.95	19.99	51.94	17.02	3.11
CBO1	no activity							
CB2	33.69	0	46.77	32.26	20.97	53.23	17.93	1.98
CBO2	no activity							
CB3	32.93	0	45.18	33.71	21.11	54.82	18.05	2.49
CBO3	no activity							
CB4	34.01	1.42	45.12	33.57	19.89	53.46	18.18	2.41
CBO4	no activity							
CB5	32.75	1.57	46.88	31.09	20.80	51.55	16.88	3.10
CBO5	no activity							
CB8	12.01	8.96	31.84	23.38	35.82	59.20	7.11	

of surface area, the CBO1 to CBO5 catalysts had almost no activity for the OCM reaction. Comparatively, on catalysts CB1 to CB5, high catalytic activity and high C_2 hydrocarbon selectivity for OCM reaction were observed.

Table 2 shows that, when the ratios of BaF_2 to CeO_2 increased from 1 : 1 to 5 : 1, total C_2 yields of 17–18% with C_2^+ selectivity of 51% to 55% were obtained. CH_4 conversion and the selectivities of ethylene, ethane, CO and CO_2 changed very little. When the BaF_2 to CeO_2 ratios increased from 5 : 1 to 8 : 1, CH_4 conversion decreased rapidly, and the selectivities of $C_2^=$ and CO_2 also decreased, while the ethane and total C_2 selectivities increased rapidly.

From the data in table 2 we found that there was no direct relationship between the specific surface area and the catalytic properties of the catalysts. Probably the change of surface area in these catalysts was too small to cause observable changes in catalytic activity and C_2 selectivity.

These results suggested that, with the increase of BaF_2/CeO_2 ratios from 5 : 1 to 8 : 1, the concentration of active centers on the surface decreased, and there were not enough active centers to activate methane and catalyze the oxidative dehydrogenation of ethane to ethylene; at the same time, the deep oxidation of hydrocarbons was also partially inhibited.

3.1. THE EFFECT OF OPERATING CONDITIONS ON CATALYTIC PROPERTIES

The influence of reaction temperature on CH_4 conversion and selectivities of C_2H_4 over CB1 is shown in fig. 1. The results indicate that, below 680°C, the activity and C_2 selectivity were very low (CH_4 conversion < 8%, C_2 selectivity < 16%), and the principal product was CO_2 (selectivity > 82%). When temperature increased from 680 to 700°C, CH_4 conversion increased from 8 to 34.0%, C_2 selectiv-

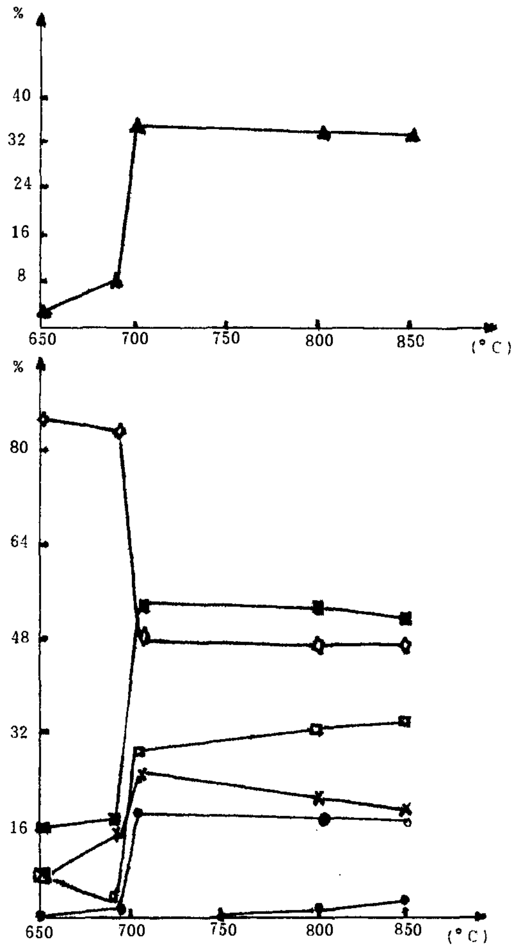

Fig. 1. The relationship between catalytic properties and reaction temperature on CeO_2/BaF_2 (1 : 1) (GHSV = 15000 h^{-1}, $CH_4 : O_2 = 2.3 : 1$). (▲) CH_4 conversion, (■) C_2 selectivity, (◇) CO_2 selectivity, (●) CO selectivity, (□) ethylene selectivity, (×) ethane selectivity, (○) C_2 yield.

ity increased from 16 to 54.4%, and the selectivity of CO_x decreased from 82 to 45.6%. Within the temperature region of 700–850°C, CH_4 conversion, C_2 selectivity and CO_2 selectivity slightly decreased (about 0.8–1.6%), and CO selectivity increased from 0 to 3%. At the same time, the selectivity of ethane decreased, while the selectivity of ethylene increased. This result indicated that high temperature favors the dehydrogenation of ethane to ethylene. Fig. 1 also shows that catalyst CB1 has a relatively wide operating temperature (700–850°C) region. In this temperature region, CH_4 and C_2 selectivity remained almost unchanged.

Fig. 2 shows the reaction results over CB1 at different CH_4 to O_2 ratios. With increasing CH_4 to O_2 ratio, CH_4 conversion, C_2 yield, and the selectivities of ethylene, CO_2 and carbon monoxide decreased, while the selectivity of ethane and total C_2 products increased rapidly. This result elucidated that ethane was the principal

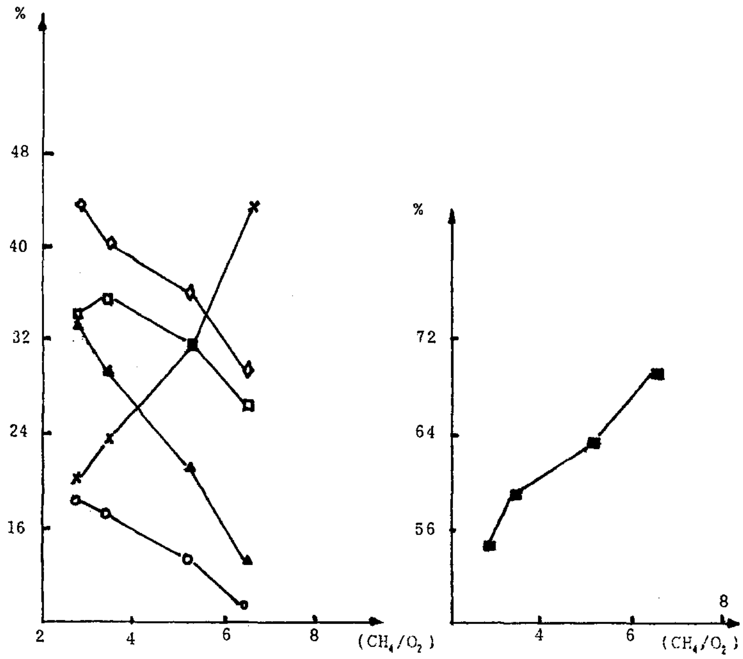

Fig. 2. The effect of CH_4 to O_2 ratio on catalytic properties on CeO_2/BaF_2 (1 : 1) (800°C, GHSV = 15000 h^{-1}). (▲) CH_4 conversion, (■) C_2 selectivity, (◇) CO_2 selectivity, (□) ethylene selectivity, (×) ethane selectivity, (○) C_2 yield.

primary product of OCM, and ethylene might come mostly from the oxidative dehydrogenation of ethane. At high CH_4 to O_2 ratio, CH_4 was first oxidatively dimerized to ethane; since there is not enough O_2 to oxidize ethane to ethylene and deeply oxidize C_2H_4, C_2H_6 and intermediate hydrocarbon species, the total CO_x selectivity was low, and a relatively higher total C_2 selectivity could be obtained.

3.2. STRUCTURE ANALYSIS AND IONIC EXCHANGE IN CeO_2/BaF_2

The XRD measurement showed that, when the molar ratios of CeO_2/BaF_2 changed from 1 : 1 to 1 : 5, only CeO_2 and BaF_2 phases were detected in the catalysts (tables 3 and 4). But the lattice of BaF_2 contracted (table 3), while that of CeO_2 expanded (table 4). These results indicated that partial anionic and/or cationic exchange between BaF_2 and CeO_2 lattices, in other words isomorphous substitution, occurred.

In the case when one O^{2-} substituted for one F^- in the BaF_2 lattice, there would be one more electron on the oxygen, forming an "electron-enriched lattice oxygen". Generally, such kind of "electron-enriched lattice oxygen" easily donates an electron to form O^- species to maintain the electric neutrality of the lattice. In this case, the donated electron may be bound on Ce^{4+} centers and generate a partially reduced state of Ce^{4+}. These centers might be also formed by the substitution of one F^- for one O^{2-} in the CeO_2 lattice. On the other hand, if one O^{2-} substituted

Table 3
XRD results of BaF_2 phase in catalysts

Catalyst		(111)	(200)	(220)	(311)	(331)	(422)
CB1	d (Å)	3.556	3.074	2.178	1.855	1.411	1.256
	I/I_0	73	22	63	46	18	16
CB2	d (Å)	3.559	3.089	2.177	1.856	1.411	1.257
	I/I_0	100	44	90	60	21	22
CB3	d (Å)	3.582	3.097	2.188	1.863	1.415	1.257
	I/I_0	100	27	52	36	11	9
CB4	d (Å)	3.562	3.079	2.173	1.852	1.407	1.253
	I/I_0	100	29	54	36	10	7
CB5	d (Å)	3.565	3.083	2.170	1.853	1.421	1.253
	I/I_0	100	29	50	37	5	9
pure	d (Å)	3.579	3.100	2.193	1.870	1.423	1.266
BaF_2	I/I_0	100	27	79	51	13	14

for two F^- in the BaF_2 lattice, anion vacancies might be formed. The possible formation of O^- ions (which are smaller in size than F^-) and anion vacancies would lead to the contraction of the BaF_2 lattice. In addition, the substitution of Ce^{4+} for Ba^{2+} in BaF_2 could also bring about the contraction of the BaF_2 lattice. If two F^- were substituted for one O^{2-} or Ba^{2+} for Ce^{4+} in CeO_2 lattice, the lattice of CeO_2 might expand. In the following section, more experimental evidence will be provided to verify the above suggestions.

3.3. THE OXYGEN ACTIVATION OVER CeO_2/BaF_2

3.3.1. XPS characterization

After CeO_2/BaF_2 (1 : 2) was pretreated as described in the experimental section

Table 4
XRD results of CeO_2 phase in catalysts

Catalyst		(111)	(200)	(220)	(311)	(222)	(400)	(331)
CB1	d (Å)	3.121	2.707	1.911	1.630	1.563	1.354	1.241
	I/I_0	100	37	82	67	12	10	223
CB2	d (Å)	3.129	2.711	1.916	1.6335	1.566	1.354	1.243
	I/I_0	71	26	53	40	7	10	20
CB3	d (Å)	3.142	2.719	1.918	1.635			
	I/I_0	46	14	23	14			
CB4	d (Å)	3.136	2.714	1.916	1.634	1.564		1.243
	I/I_0	18	5	9	6	2		3
CB5	d (Å)	3.140	2.715	1.917				
	I/I_0	17	7	10				
pure	d (Å)	3.1234	2.7056	1.9134	1.6318	1.5622	1.3531	1.2415
CeO_2	I/I_0	100	30	52	42	8	8	

and adsorbed with oxygen, the XPS spectra showed that, compared to CeO_2, the binding energy of Ce $3d_{5/2}$ in CeO_2/BaF_2 (1 : 2) decreased by about 2.2 eV (fig. 3). This result suggested that quasi-free electrons or a partially reduced state of Ce^{4+} were formed, and indicated that the introduction of CeO_2 into BaF_2 enhanced the electron donating ability of catalysts. The XPS analysis also showed that, compared to BaF_2, no change in the binding energies of F^- and Ba^{2+} in the catalyst was observed. Increase of the electron donating ability of catalysts should favor the adsorption and activation of molecular O_2.

The O 1s spectrum (fig. 4) on O_2 adsorbed CeO_2/BaF_2 (1 : 2) can be resolved into four peaks with BE of 527.1, 528.9, 530.4 and 531.9 eV respectively, while the corresponding spectrum on pure CeO_2 showed only one peak at 529.1 eV. The peaks at 527.1, 528.9, and 529.1 eV were attributed to lattice oxygen O^{2-} [7,8]. The peak at 531.9 eV might be assigned to O^-, O_2^{2-} or/and O_2^- ions located in different chemical environments [8,9]. The peak at 530.4 eV might also arise from O^{2-} ions located in different sites [10,11]. The binding energy of O^{2-} at 527.1 eV is lower than the normal value (528–529 eV) of lattice oxygen ions (O^{2-}), and might be attributed to the "electron-enriched lattice oxygen".

Under the reaction conditions, both the "electron-enriched lattice oxygen" and

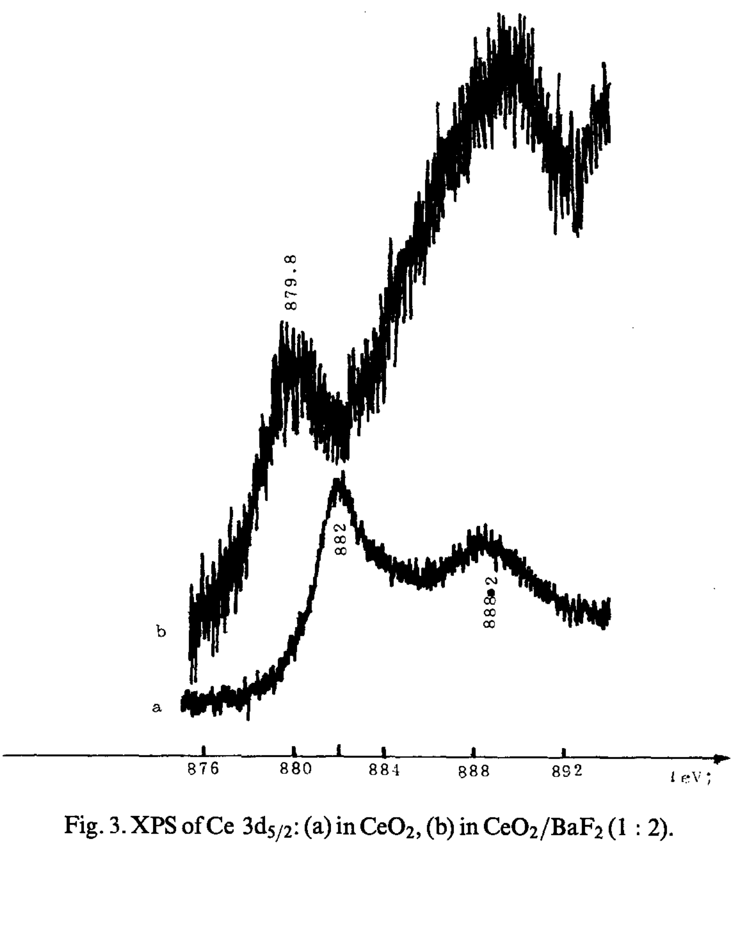

Fig. 3. XPS of Ce $3d_{5/2}$: (a) in CeO_2, (b) in CeO_2/BaF_2 (1 : 2).

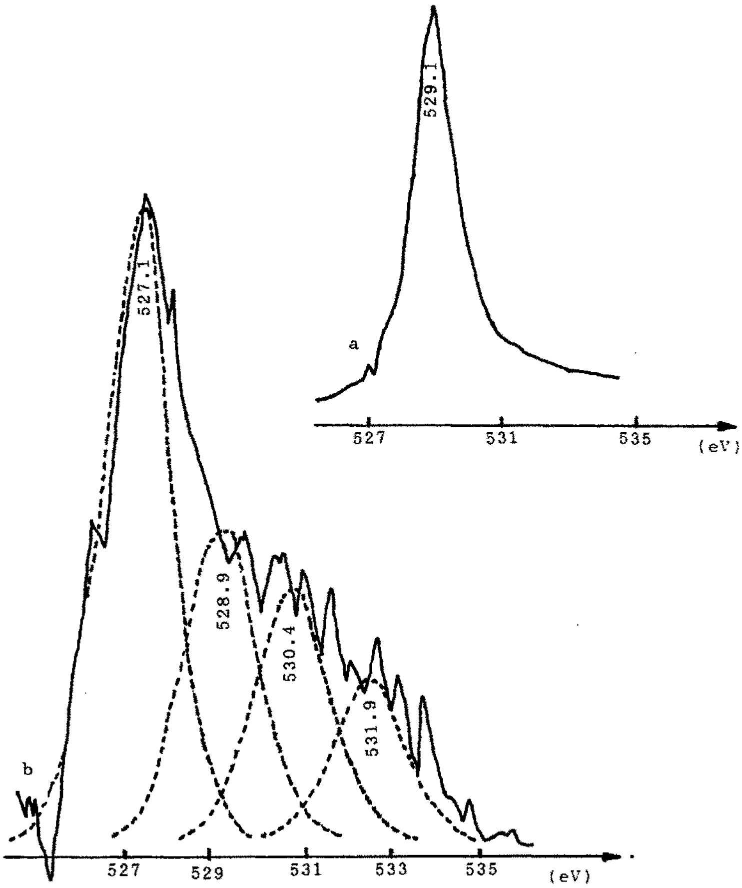

Fig. 4. XPS of O 1s: (a) O_2 adsorbed CeO_2, (b) O_2 adsorbed CeO_2/BaF_2 (1 : 2).

quasi-free electrons may react with O_2 to generate nonfully reduced oxygen species, as shown in scheme 1.

$$\underset{\text{e}^-\text{-enriched}}{O^{2-}} + O_2 \longrightarrow O^- + O_2^-$$

$$\xrightarrow{O^-} O_2^{2-} + O^-$$

$$e^- + O_2 \longrightarrow O_2^- \xrightarrow{e^-} O_2^{2-} \rightleftharpoons 2O^-$$

Scheme 1.

3.3.2. Raman characterization

On both the O_2 adsorbed and degassed CeO_2 samples, no Raman bands were observed between 600 and 1500 cm^{-1}. On degassed CeO_2/BaF_2 (1 : 2), we also did

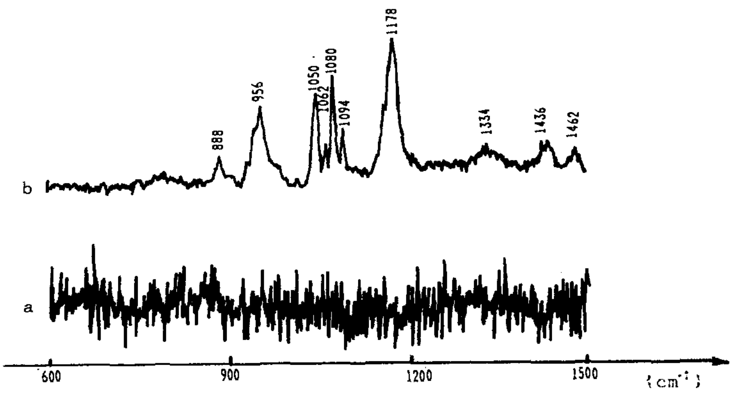

Fig. 5. Raman spectra of CeO_2/BaF_2 (1 : 2): (a) degassed sample, (b) O_2 adsorbed sample.

not observe any Raman peaks within the same region (fig. 5). But on O_2 adsorbed CeO_2/BaF_2 (1 : 2), Raman bands at 888, 956, 1050, 1062, 1080, 1094, 1178, 1334, 1436 and 1462 cm^{-1} were observed and assigned to dioxygen adspecies on the catalysts. The bands at 888 and 956 cm^{-1} may be assigned to O_2^{2-} ions [7,8,12,13]. The bands with wave numbers between 1050 and 1178 cm^{-1} fall in the vibration region of O_2^- ions, and are assigned to O_2^- ions [14–17]. The bands at 1334, 1436 and 1462 cm^{-1} might arise from the adsorbed oxygen molecule with less negative charge [15,18,19].

The wave numbers of the bands at 888 and 956 cm^{-1} are higher than the common value 850 cm^{-1} of O_2^{2-} ions [10,21]. This might result from perturbation of O_2^{2-} ions by the strong electrostatic force of the quasi-ionic solid, which would give bands with higher wave numbers than the common values, because partial electron withdrawal from the antibonding orbitals of O_2^{2-} would enhance the O–O bond, as suggested by Al-Mashta et al. [15].

The wave numbers between 1050 and 1094 cm^{-1} are lower than the general values (around 1100 cm^{-1}) of O_2^- ions [22,23–27]. Che and Tench have suggested that backdonating of electrons from the metal orbitals to the antibonding orbitals of oxygen will decrease the V_{00} frequency of the dioxygen species [28]. In the co-condensation reaction of Ag with $^{16}O_2/Ar$ matrix, Mcintosh et al. [26] also observed the low vibration band at 1097 cm^{-1}. Tsyganenko et al. [17] observed the IR band of O_2^- ions at 1070 cm^{-1} on NiO. Zecchina et al. [28,29] detected IR bands between 1015 and 1160 cm^{-1} on MgO–CaO, and assigned them to O_2^- ions located in different chemical environments. In the case of a CeO_2/BaF_2 catalyst, the backdonating bond between partial reduced cerium ions and dioxygen adspecies might also form, and the Raman bands from 1050 to 1094 cm^{-1} can therefore be assigned to the vibrations of O_2^- ions located in different chemical environments [30].

The band at 1178 cm^{-1} is close to the IR bands around 1180 cm^{-1} observed by Davydov et al. [16] on O_2 adsorbed TiO_2, and could be assigned to O_2^- ions. However, the bands at 1334, 1436, and 1462 cm^{-1} have much higher wave numbers than that of normal O_2^- ions. The vibration band of adsorbed neutral O_2 species was known falling in the range of 1460–1700 cm^{-1} [9,31–33]. Combining the reported work with that of Al-Mashta et al. [15], we tentatively assigned the Raman bands between 1334 and 1462 cm^{-1} to $O_2^{\delta-}$ intermediates between O_2^- and O_2.

The ESR spectra of catalysts are shown in fig. 6, on degassed catalysts CeO_2/BaF_2 (1 : 2). ESR signals with g values of 2.0736, 2.0439 and 2.0208 were observed. These g values were assigned to O^- ions in the bulk of catalysts, since no multinuclear paramagnetic oxygen species, such as O_2^-, and O_3^- can stably exist under the sample treatment conditions described in the experimental section, and Raman bands of O_2^- and O_3^- ions were not detected on the degassed sample in the above Raman experiment.

When O_2 was passed through the degassed CeO_2/BaF_2 (1 : 2) sample, different ESR signals (fig. 6) with g values of 2.2377, 2.1807, 2.1544, 2.1182, 2.0832 and 2.0573 were observed. Since paramagnetic O_3^- species may be unstable at room temperature [34–36], the above ESR signals were assigned to O_2^- ions. The reason for the disappearance of the ESR signals on degassed samples under O_2 exposure might be that, when O_2 adsorbed on the catalyst, the original quasi-free electrons or "electron-enriched lattice oxygen (O^{2-})" might react with O_2 molecules, as shown in scheme 1, thereby increasing the concentration of O^- ions in the catalysts. If the distance between two O^- ions decreased to a certain value, two O^- ions might couple forming O_2^{2-} ions, leading to the disappearance of ESR signals of O^- ions.

4. Conclusion

Based on the above results, we may conclude that, with the addition of BaF_2 to CeO_2 and treatment in air at 900°C, anionic and/or cationic exchange between metal oxide and metal fluoride lattices took place to some extent, leading to the for-

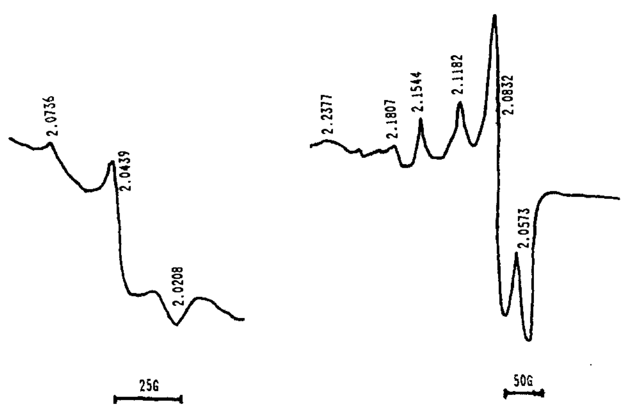

Fig. 6. ESR spectra of CeO_2/BaF_2 (1 : 2): (a) degassed sample, (b) O_2 adsorbed sample.

mation of anion vacancies, O^- ions, quasi-free electrons, "electron-enriched lattice oxygen" species, as well as expansion and contraction of the CeO_2 and BaF_2 lattices, respectively. These factors should be responsible for the significant improvement of the catalytic performance. In consideration of the stronger electronegativity of F than O, the catalyst containing F^- might be more conducive to the formation of oxygen species with less negative charge, which favors the selective conversion of CH_4 to C_2 hydrocarbons. On the other hand, the dispersion of "inert" fluorides on the catalyst surface will be also beneficial to the isolation of the surface active centers and decrease of CO_2 inhibition, and will therefore be favorable to the improvement of C_2 selectivity and the lowering of the activation energy.

References

[1] K. Wohlfahrt, M. Bergfeld and H. Zengel, German Patent 3503664 (1986).
[2] T.R. Baldwin, R. Burch, E.M. Crabb, G.D. Squire and S.C. Tsang, Appl. Catal. 56 (1989) 219.
[3] R. Burch, G.D. Squire and S.C. Tsang, Appl. Catal. 43 (1988) 105;
R. Burch, G.D. Squire and S.C. Tsang, Appl. Catal. 46 (1989) 69.
[4] X.P. Zhou, S.Q. Zhou, S.J. Wang, J.X. Cai, W.Z. Weng, H.L. Wan and K.R. Tsai, Chemical Research in Chinese Universities 9 (1993) 264.
[5] X.P. Zhou, W.D. Zhang, H.L. Wan and K.R. Tsai, Catal. Lett. 21 (1993) 113.
[6] X.P. Zhou, Z.S. Chao, S.J. Wang, W.Z. Weng, H.L. Wan and K.R. Tsai, *The 4th China–Japan Bilateral Symposium on Effective Utilization of Carbon Resources*, Dalian, October 1993, p. 37.
[7] J.L. Gland, B.A. Sexton and G.B. Fisher, Surf. Sci. 95 (1980) 587.
[8] B.A. Sexton and R.J. Madix, Chem. Phys. Lett. 76 (1980) 294.
[9] A.A. Davydov, Kinet. Katal. 20 (1979) 1506.
[10] Y. Inoue and I. Yasumori, Bull. Chem. Soc. Jpn. 54 (1981) 1505.
[11] X.D. Peng and D.C. Stair, J. Catal. 128 (1991) 264.
[12] A. Metcalfe and S. Ude Shanker, J. Chem. Soc. Faraday Trans. I 76 (1980) 630.
[13] C. Backx, P.P.M. de Groot and P. Biloen, Surf. Sci. 104 (1981) 300.
[14] D.W.L. Griffiths, H.E. Hallam and W.J. Thomas, J. Catal. 17 (1970) 18.
[15] F. Al-Mashta, N. Sheppard, V. Lorenzelli and G. Busca, J. Chem. Soc. Faraday Trans. I 78 (1982) 979.
[16] A.A. Davydov, M.P. Komarova, V.F. Anufrienko and N.G. Maksimov, Kinet. Katal. 14 (1973) 1519.
[17] A.A. Tsyganenko, J.A. Rodionova and V.N. Filimonov, React. Kinet. Catal. Lett. 11 (1979) 113.
[18] A.B.P. Lever, G.A. Ozin and H.B. Gray, Inorg. Chem. 19 (1990) 1823.
[19] J.S. Valentine, Chem. Rev. 73 (1973) 237.
[20] A. Metcalfe and S. Ude Shankar, J. Chem. Soc. Faraday Trans. I 76 (1980) 630.
[21] B.A. Sexton and R.J. Madix, Chem. Phys. Lett. 76 (1980) 294.
[22] C. Li, K. Domen, K. Maruya and T. Onishi, J. Chem. Soc. Chem. Commun. (1988) 1541.
[23] L. Andrews, J.T. Hwang and C. Trindle, J. Phys. Chem. 77 (1973) 1065.
[24] R.R. Smardzewski and L. Andrews, J. Phys. Chem. 77 (1973) 801.
[25] R.R. Smardzewski and L. Andrews, J. Chem. Phys. 57 (1972) 1327.
[26] D. Mcintosh and G.A. Ozin, Inorg. Chem. 16 (1977) 59.
[27] C. Li, K. Domen, K.I. Maruya and T. Onishi, J. Am. Chem. Soc. 111 (1989) 7683.

[28] A. Zecchina, G. Spoto and S. Coluccia, J. Mol. Catal. 14 (1982) 351.
[29] E. Giamello, Z. Sojka, M. Che and A. Zecchina, J. Phys. Chem. 90 (1986) 6084.
[30] C. Li, K. Domen, K.I. Maruya and T. Onishi, J. Am. Chem. Soc. 111 (1989) 7683.
[31] A.A. Tsyganenko and V.N. Filimonov, Spectrosc. Lett. 13 (1980) 583.
[32] A.A. Tsyganenko, T.A. Rodionova and V.N. Filimonov, React. Kinet. Catal. Lett. 11 (1979) 113.
[33] H. Forster and M. Schuldt, J. Chem. Phys. 66 (1977) 5237.
[34] M. Iwamoto, Y. Yoda, N. Yamazoe and T. Seiyama, J. Phys. Chem. 82 (1978) 2564.
[35] T. Ito, Masayokato, K. Toi, T. Shirakawa, I. Ikemoto and T. Tokuda, J. Chem. Soc. Faraday Trans. I 81 (1985) 2835.
[36] T. Ito, M. Yoshioka and T. Tokuda, J. Chem. Soc. Faraday Trans. I 79 (1983) 2277.